Electronic structure of UPt_3

R. C. Albers and A. M. Boring
Materials Science and Technology Division, Los Alamos National Laboratory, Los Alamos, New Mexico 87545

N. E. Christensen
Max-Planck-Institut für Festkörperforschung, D-7000 Stuttgart 80, Federal Republic of Germany and Center for Material Science, Los Alamos National Laboratory, Los Alamos, New Mexico 87545*
(Received 4 November 1985)

Fully relativistic linear muffin-tin orbital electronic band-structure results are presented for UPt_3 in the experimentally observed hexagonal $SnNi_3$ crystal structure. The basic electronic structure is a narrow spin-orbit-split U $5f$ band at the Fermi energy just above a filled Pt $5d$ band. Hybridization between the two bands removes states from the top of the Pt $5d$ band and places them in the energy region of the U $5f$ band. Besides a discussion of hybridization, the total and projected density of states, and bonding, comparison calculations with a different exchange-correlation potential and where three U $5f$ states have been forced into the core (to simulate localized states) are also presented. In the latter case U $5f$ hybridization changes the Pt d-band bonding and causes the pressure to increase more than would be expected by a loss of f-electron bonding only. Thus itinerant U f character has important observable effects on the transition-metal d band. To better understand the effects of hybridization, of the transition-metal d band, and of the local crystalline symmetry, band-structure calculations of UIr_3, UPt_3, and UAu_3 in the cubic $AuCu_3$ structure are shown and discussed, as well as calculations for pure fcc U and Pt metal. Compared with UIr_3, UPt_3 has a much weaker U f and transition-metal d hybridization and in this respect more closely resembles the filled d-band case of UAu_3.

I. INTRODUCTION

The heavy-fermion material UPt_3 has many unusual and interesting physical properties that are almost surely dominated by its electronic structure. This is most obvious in its specific heat,[1,2] which has an enhanced linear electronic specific-heat coefficient γ of 452 mJ(mole U)$^{-1}$K^{-2} that is 2 orders of magnitude larger than typical metals and about a factor of 20 larger than most band-structure predictions.[3–8] Strong electron-electron correlations also manifest in a $T^3 \ln T$ term in the low-temperature specific heat,[2,9] which is believed to be due to spin fluctuations. This latter interpretation has recently been supported by neutron scattering.[10,11] At low temperatures UPt_3 is a superconductor,[2] with a T_c of 0.54 K. Because of the apparent simultaneous presence of both spin fluctuations and superconductivity (as well as for other reasons), the idea that UPt_3 may be a p-wave or triplet superconductor analogous to the p-wave superfluid phases of the liquid ^{3}He has been raised.[2,9,12–15]

At the present time, the low-temperature ground state of UPt_3 seems unique. Although it shares some similarities with other heavy-fermion systems such as a Curie-Weiss-like magnetic susceptibility[1,16–18] at high temperatures, it is quite different from the other two known heavy-fermion superconductors, UBe_{13} and $CeCu_2Si_2$. For example, the specific heat of UPt_3, besides having a γ about half as big as that of the other two,[12,19] has the additional $T^3 \ln T$ term. Its electrical resistivity[2] decreases monotonically as the temperature is lowered like a normal metal, whereas the other two systems[12,20] (which are more similar to each other) show a far more complex temperature dependence. With a hexagonal structure (UBe_{13} is cubic) it exhibits strong anisotropies in its magnetic susceptibility,[1] superconducting upper critical field,[21] and ultrasonic attenuation.[22]

To place UPt_3 in perspective, one should note the wide variation in the physical properties of the heavy-fermion materials.[9,23,24] While by definition all these materials have huge specific-heat enhancements, some are superconducting, some are magnetic, and some, at least to the lowest temperatures so far investigated, are neither. At present no one knows how to predict which materials will fall in each subcategory. Since all are presumably dominated by the electronic structure that is responsible for the specific-heat enhancements, it is useful to examine the different factors that may influence the electronic structure in hopes of finding some systematic features that would help explain their differences. One possible starting point is crystal structure and one may immediately focus on three different aspects of the crystalline order in these materials: (i) the nearest f-atom to f-atom separation, (ii) the types of atoms surrounding each f-atom site, and (iii) the symmetry of the crystal around the f-atom sites.

Meisner *et al.*[25] have attempted to empirically correlate the f-atom spacing with the specific heat. From the Hill plots[26] normal itinerant f-band behavior is expected for small f-atom separation ($\lesssim 3.4$ Å for U), where the f orbitals have a significant direct overlap. At larger spacings one would intuitively expect the bands to narrow and for electron-electron correlations to cause the f orbitals to lo-

calize into magnetic states (for partially filled shells). The heavy-fermion materials, of course, are precisely those materials that have large f-atom separations and should have become magnetic but do not. Meisner *et al.*[25] have plotted the electronic specific-heat coefficient γ versus f-atom spacing for many heavy-fermion systems and show that those materials with the largest γ for a given f-atom spacing falls on a smooth curve (actually two different curves, one for uranium compounds and one for cerium compounds). While there are many systems that lie below these curves (i.e., that have smaller γ's at a fixed spacing), the most interesting heavy-fermion systems (e.g., superconductors and magnets) tend to fall on the highest γ curve. Put another way, those materials with the highest γ's for any given spacing are those materials for which the effects of the narrow f bands are the strongest and hence are the most different from ordinary metals. This correlation, while it provides an empirical guide for experimentalists to suggest which heavy-fermion materials should be most carefully and exhaustively studied, provides no understanding of why different materials, which may have nearly the same f-atom spacing, should have such different γ's or physical properties.

Since the f states at these large separations cannot form bands through direct overlap,[27] the hybridization of the f states with neighboring atoms must be extremely important for determining the different γ's and behavior at any given f-atom separation. As we have remarked in earlier work,[28,6] for the heavy-fermion superconductors the dominant hybridization seems to be with broad s-p bands originating on neighboring atomic sites. Clearly much further work needs to be done to identify the specific nature of the interaction with the neighboring atoms that cause so much diverse behavior in these systems.

Besides f-atom separation and the type of atoms nearby, the local symmetry surrounding the f atoms could also be significant for heavy-fermion behavior. One may speculate, e.g., that the hybridization could be drastically altered (all other things being kept the same) if the local symmetry is changed. By comparing calculations between the experimentally observed hexagonal $SnNi_3$ crystal structure and an hypothetical cubic $AuCu_3$ structure, which only differ in the way the planes of atoms stack (in analogy with the difference between an hcp and an fcc lattice), we can test for hybridization changes between hexagonal and cubic symmetry for UPt_3, at least at the one-electron level. Comparison with an fcc lattice for a pure element is also of interest because an fcc crystal structure results if all atoms in a $AuCu_3$ structure are identical.

As we have already mentioned, because the low-temperature exotic behavior of heavy-fermion materials in general and UPt_3 in particular exist in the presence of strong electronic enhancements, the electronic structure must play a dominant role. We therefore expect the strongly renormalized ground state to have important many-body electron-electron correlations that are not included in usual density-functional electronic-band-structure calculations. For this reason, while a band-structure approach cannot be expected to explain in detail the low-temperature properties of UPt_3, e.g., specific heat, magnetic susceptibility, electrical resistivity, and other such properties, nonetheless, it is the only *a priori* theory of electronic structure currently available and provides a useful framework from which to start. Besides providing useful information on approximate band placements, bandwidths, hybridization, and spin-orbit and crystal-field splittings, as well as an accurate picture of the one-electron electronic structure, the symmetry of the underlying crystal lattice is built in from the very beginning, unlike most phenomenological many-body theories. Moreover, at elevated temperatures ($\gg$30 K, for example), where thermal fluctuations may destroy the effects of the many-body correlations, a one-electron approach may better describe experiment. Finally, we note that the band structure provides a useful reference from which to estimate the strength of the many-body enhancements (λ in the specific heat, for example) and is appropriate for the non-f bands.

Our main focus in this paper will therefore be to understand the one-electron model of UPt_3 in as great detail as possible. In Sec. II we will discuss the technical aspects of our calculations and describe the crystal structure of UPt_3. In Sec. III we will discuss the basic one-electron electronic structure, i.e., the general placement of the energy bands, the total and projected density of states of UPt_3, comparisons and differences with pure fcc U and Pt at the same average density, hybridization, and the effects of the spin-orbit interaction. In Sec. IV we discuss other aspects of the electronic structure such as comparison calculations where three U f electrons are put in the core, placement of the Fermi energy, differences due to the local exchange-correlation potential used, and effects of the structural geometry. In Sec. V we discuss bonding properties of UPt_3, and in Sec. VI compare UPt_3 with UIr_3 and UAu_3 calculations. A general summary and discussion will be presented in Sec. VII.

II. METHOD

The electronic band-structure results presented in this paper were obtained by the Dirac fully relativistic linear muffin-tin orbitals (LMTO) method,[29–41] mostly in the atomic-sphere approximation (ASA). The observed $SnNi_3$ crystal structure of UPt_3 is sufficiently close packed for the ASA to be an excellent approximation and the effects of the combined correction term are almost negligible. The Barth-Hedin exchange-correlation potential[42] was used. For calculations in the $AuCu_3$ crystal structure, the band structure was first converged for 35 **k** points in the irreducible wedge and the mesh was then increased to 80 **k** points. The $SnNi_3$ crystal structure calculations were first converged for 40 **k** points in the irreducible wedge and then increased to 84 **k** points.

Because the U 5f bands near the Fermi energy E_F show so much structure, it is important to use a large number of **k** points in the irreducible wedge to determine detailed features of the density of states (DOS) in that energy regime. Hence, although the lower number of **k** points for each crystal structure seemed to be sufficient for generating the self-consistent potential, one final iteration was done with 126 **k** points for the $SnNi_3$ structure for a more accurate density of states. The tetrahedron method[43,44]

was used to evaluate the density of states. For the conduction band, the DOS was calculated at 1 mRy ($\approx$0.0136 eV) intervals. All the DOS plots shown in this paper draw straight-line segments between each calculated value.

Another technical problem that UPt_3 shares with most actinide, rare-earth, and other large-Z systems is that some of the core states just below the conduction band often sufficiently overlap to have a significant bandwidth. For UPt_3 about 4.2% of each atomic U $6p$ orbital extends beyond the uranium atomic-sphere radius (3.0488 bohrs) and the U $6p_{1/2}$ and $6p_{3/2}$ bandwidths are 3 and 40 mRy, respectively. The final UPt_3 calculations were therefore done using two panels—one panel (or separate LMTO calculation) to determine the U $6p$ states (treated as energy bands) and a second panel for the conduction bands. The remaining core charge was frozen and taken from isolated atom calculations. For the lower panel s-p-d angular momentum components were included in the basis and in the upper panel s-p-d-f components. In each case the uranium and platinum atoms had the same number of angular-momentum components. Because of the small bandwidths, we evaluated the DOS for the lower panel at 0.5 mRy intervals. Since the LMTO technique depends on a parametrization of the logarithmic derivatives that is only accurate around fixed linearization energies for each angular-momentum component (or κ component for the fully relativistic calculations), it is important to do separate calculations for each set of bands. Attempts to include both the U $6p$ states and the conduction bands in one giant panel such as that reported in Ref. 8 might be expected to give poor results because such a large energy range is involved. Nonetheless, a test that we performed shows that this approach gives reasonably accurate results for UPt_3, since the occupied part of the conduction band has almost no uranium p character.

For calculations in which the U $6p$ states are treated as core states, consideration must be given to those parts of the atomic wave functions that extend beyond the atomic-sphere radius. In all calculations reported in this paper, we have followed the standard practice of leaving alone those parts of the core wave functions that are inside the atomic sphere and redistributing any core charge that falls outside as a constant charge density inside the atomic sphere. This was also done for calculations where we forced the U $5f$ states to be corelike (with about 4.4% of each U $5f$ orbital extending beyond the uranium atomic-sphere radius). All core orbitals were taken to be those of the isolated atom.

The band structure, of course, also depends on the crystal structure. For UPt_3 the experimentally observed crystal structure is in the $SnNi_3$ (DO 19) structure (sometimes also referred to as a $MgCd_3$ structure). In crude terms this is the hexagonal modification of the cubic $AuCu_3$ structure; the major difference between the two structures is a slightly different stacking of the planes in much the same way that the hcp and fcc structures differ. In the $SnNi_3$ crystal structure for UPt_3, there are two equivalent U sites and six equivalent Pt sites in the unit cell. As shown in Fig. 1, each U atom has three Pt atoms sitting in a triangular configuration in planes $\frac{1}{2}c$ above and below

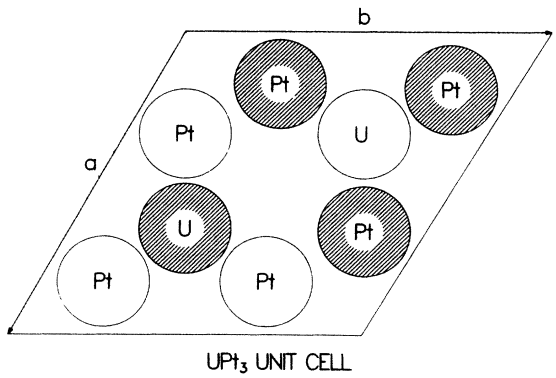

FIG. 1. Sketch of the atomic positions for UPt_3 in the $SnNi_3$ crystal structure. The vectors **a** and **b** are the lattice vectors in the x-y plane of the real space unit cell for a hexagonal lattice. The open circles are in a plane $z=c/4$ and the shaded circles at $z=(\frac{3}{4})c$. We have added a dashed line which breaks up the unit cell into two pieces to assist in visualizing the unit cell.

it. In the same plane as the U atom there are three Pt atoms in the other half of the cell. The nearest Pt atoms in this plane are almost at the same distance as those in the planes above and below. As is usual for hexagonal stackings, each platinum atom is directly above and below platinum atoms in adjacent planes of platinum atoms. In terms of the hexagonal basis vectors for the unit cell **a**, **b**, and **c**, the uranium atoms are located at $(\frac{1}{3},\frac{2}{3},\frac{1}{4})$ and $(\frac{2}{3},\frac{1}{3},\frac{3}{4})$, and the platinum at $(x,2x,\frac{1}{4})$, $(2\bar{x},\bar{x},\frac{1}{4})$, $(x,\bar{x},\frac{1}{4})$, $(\bar{x},2\bar{x},\frac{3}{4})$, $(2x,x,\frac{3}{4})$, and $(\bar{x},x,\frac{3}{4})$. The parameter x requires x-ray intensity calculations for it to be determined by x-ray diffraction measurements and as far as we know has never been determined for UPt_3. In the absence of this information we have used the ideal value of the parameter $x=\frac{5}{6}$. With this value for x, the interatomic distances between the uranium and platinum atoms are reported in Ref. 45. For our calculations we have used the slightly different lattice constants:[46] $a=b=5.76390$ Å, $c=4.90270$ Å, and hence $c/a=0.8506$. If c/a were set equal to 0.8165, then the six Pt nearest neighbors on the same plane and the six Pt nearest neighbors on the planes above and below each uranium atoms would be equidistant.

III. BASIC ELECTRONIC STRUCTURE

First, in Fig. 2 we show the rough placement of the uranium and platinum bands in UPt_3 as determined by the energy range of a negative logarithmic derivative in the self-consistent fully relativistic UPt_3 potential for each atom. The bottom and top of the appropriate bands then correspond to the energies where the logarithmic derivatives $D_\kappa(E)$ are zero and infinite, respectively. The κ label is the standard fully relativistic notation[47] for l and j. For $j=l+\frac{1}{2}$, κ is $-l-1$ and for $j=l-\frac{1}{2}$, κ is equal to l. For a pure element with one atom per unit cell this calculation is identical to using the Wigner-Seitz rules. While this procedure should be modified for compounds (see, e.g., the discussion in Ref. 48), it nonetheless often works

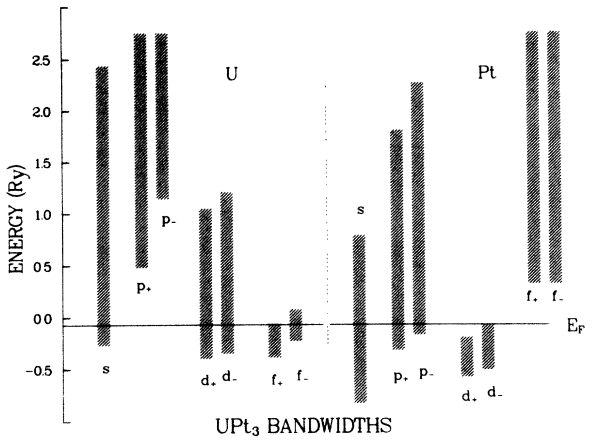

FIG. 2. Wigner-Seitz band placements for UPt_3. The left-hand side contains the U band placements and the right-hand side contains the Pt band placements. The line labeled E_F is the Fermi energy of the fully hybridized band-structure calculation. The $l+$ and $l-$ notation for $l=s,p,d$, and f refers to the two spin-orbit-split components for positive and negative κ, which corresponds to $j=l\mp\frac{1}{2}$. The band widths have been cutoff above 2.7 Ry.

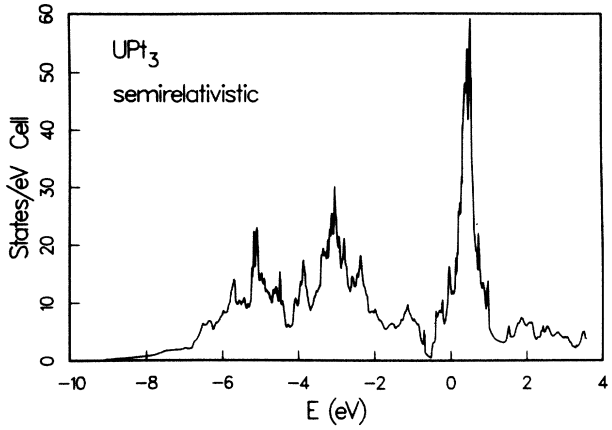

FIG. 4. Scalar-relativistic total DOS for UPt_3 in $SnNi_3$ crystal structure. The energies have been shifted so that the Fermi energy is at zero energy.

well. To place these results in context, we have also performed similar calculations for pure uranium and platinum separately (each in an fcc crystal structure with an atomic-sphere radius the same as the average atomic-sphere radius of UPt_3, 3.0488 bohrs) which are shown in Fig. 3. A comparison of Figs. 2 and 3 shows that the uranium and platinum band placements in UPt_3 are not that different from the pure metals. Since the band placements only depend on the potential at each atomic site, this implies that the potentials in UPt_3 must be similar to those of the pure metals and that differences in the band structure are mainly due to hybridization effects.

To see this in more detail it is useful to compare these band placements with density-of-states calculations of UPt_3. In Fig. 4 we show the total DOS for self-consistent semirelativistic (i.e., all relativistic effects except spin-orbit) calculations of UPt_3 and in Fig. 5 the total DOS for self-consistent fully relativistic (i.e., solutions to the Dirac equation, which include spin-orbit effects). The similarities between Figs. 4 and 5 show that the general placement of the bands is not affected by spin-orbit coupling. However, the details of the electronic structure within each band are profoundly influenced by the spin-orbit coupling. This is shown in Figs. 6 and 7, which contain, respectively, the $j=\frac{5}{2}$ and $\frac{7}{2}$ U $5f$-projected density of states (PDOS) around the uranium sites and the $j=\frac{3}{2}$ and $\frac{5}{2}$ Pt $5d$ PDOS around the Pt sites. The U $5f$ bands are clearly split into two spin-orbit subbands since the U $5f$ spin-orbit splitting is larger than the $5f$ bandwidth. This same trend is also seen from a direct examination of the bands along various symmetry directions, which are given for the fully relativistic calculations in Fig. 8. From the total DOS plots the spin-orbit splitting seems to have little effect on the Pt $5d$ bands. This is because the bandwidth

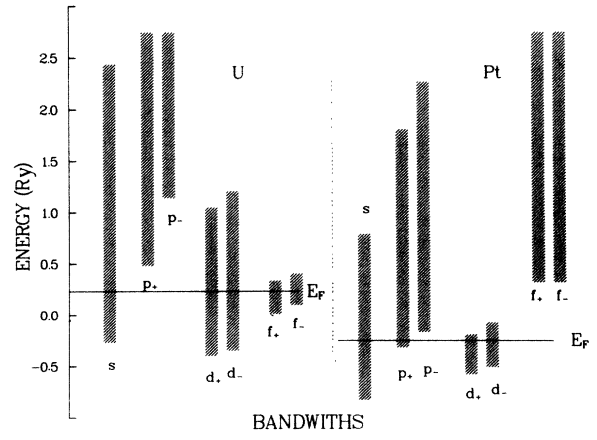

FIG. 3. Wigner-Seitz band placements for pure fcc U and Pt. The notation is the same as in Fig. 2. Because the U and Pt calculations are separate, both Fermi energies are indicated. The bands have been cut off above 2.7 Ry.

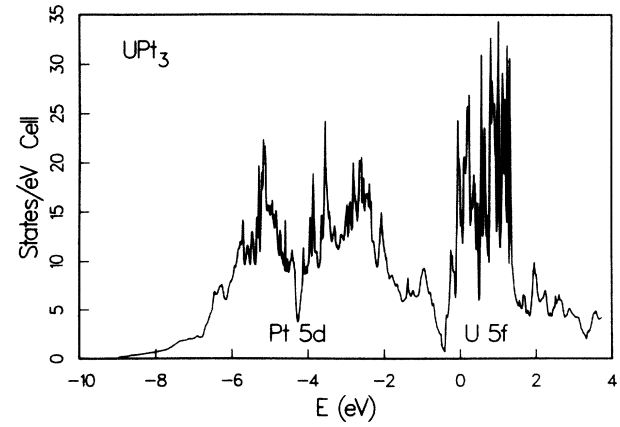

FIG. 5. Fully relativistic (including spin orbit) total DOS for UPt_3 in $SnNi_3$ crystal structure. The energies have been shifted so that the Fermi energy is at zero energy.

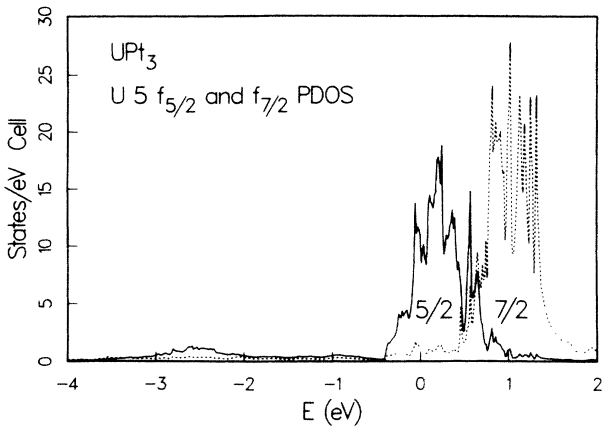

FIG. 6. The $\frac{5}{2}$ (solid line) and $\frac{7}{2}$ (dashed line) j components of the U $5f$ PDOS in UPt_3 in the $SnNi_3$ crystal structure. The energies have been shifted so that the Fermi energy is at zero energy.

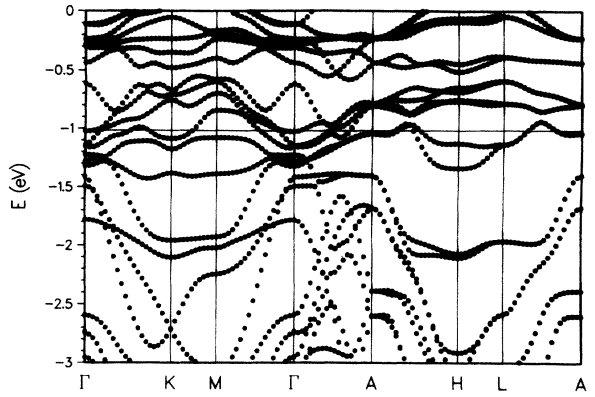

FIG. 8. UPt_3 symmetry bands with Barth-Hedin exchange-correlation potential. The horizontal line running from left to right across the figure is the Fermi energy.

is much larger than the spin-orbit splitting and hybridization between the two spin-orbit components tends to obscure the splitting. Nonetheless, the projected DOS plots of the two components of the Pt $5d$ bands in Fig. 7 clearly show the importance of spin-orbit effects on these bands. All other uranium and platinum bands are too broad to show strong spin-orbit effects in the projected DOS.

As might be expected, the pure platinum results for the Wigner-Seitz band placements are similar to those in UPt_3. The only qualitative difference is that E_F is completely above the d bands in UPt_3. On this scale a substitution of 25% U for Pt atoms seems to only slightly perturb the basic platinum band structure, which has moderately narrow $5d$ bands embedded in broad platinum $6s$ and $6p$ bands and a broad unoccupied $5f$ band that is well above the Fermi energy. Looking at finer details in the platinum projected DOS (most of which is not presented here for space considerations), we find that the $p_{1/2}$, $d_{3/2}$, and $d_{5/2}$ bands seem to be the most different between the two cases. In pure platinum the $p_{1/2}$ band seems to hybridize most strongly with the platinum $d_{3/2}$ and f states, while in UPt_3 the platinum $p_{1/2}$ DOS seems similar to the total Pt d-band DOS and shows strong hybridization with the U f bands as well as the U d-band component that is above the U f bands. It is probable that the platinum $p_{1/2}$ DOS in the Pt d-band region contains a considerable amount of hybridization with the U d-band component below E_F and that this is why its structure more closely resembles the total DOS rather than just the platinum $d_{3/2}$ component as it does in the pure metal.

Another difference in the Pt d bands is the additional structure above the main part of the bands (roughly, the energy range $-\frac{1}{2}$ to $+\frac{1}{2}$ eV in Fig. 7) which is absent in the pure metal. This additional Pt d structure obscures the hybridization gap that would be expected to be seen in the Pt d states from hybridization with the uranium d states. As we have shown in an earlier publication,[28] this extra structure is induced by hybridization with the U $5f$ bands. Additional evidence for this is provided by Fig. 9,

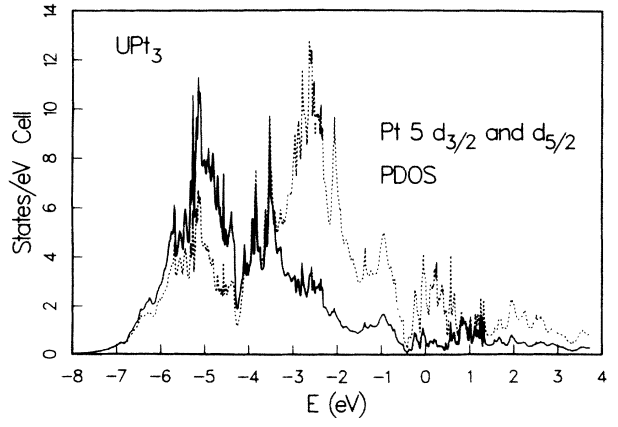

FIG. 7. The $\frac{3}{2}$ (solid line) and $\frac{5}{2}$ (dashed line) j components of the Pt $5d$ PDOS in UPt_3 in the $SnNi_3$ crystal structure. The energies have been shifted so that the Fermi energy is at zero energy.

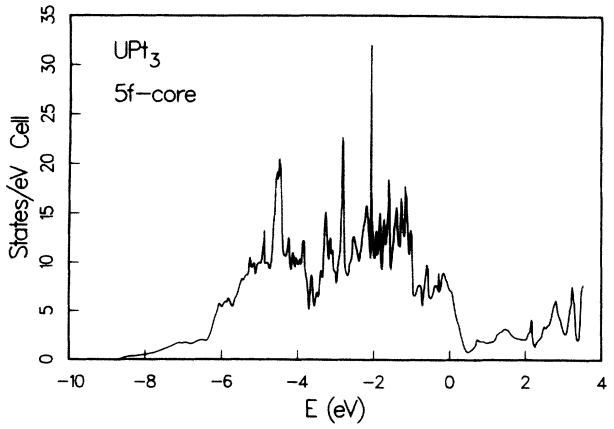

FIG. 9. Total DOS for UPt_3 in $SnNi_3$ structure with the U $5f$ electrons in the core. The energies have been shifted so that the Fermi energy is at zero energy.

which shows the total DOS for calculations where the U f electrons have been forced into the core. Above the Pt d bands there is little structure because the U f bands are missing and induce no d character in this region. There are only broad structureless bands until the U d bands turn on at higher energies.

The more interesting comparison is between the uranium band positions in the pure element and in UPt_3. Besides some small changes in the narrow U $5f$ band, the relative uranium band placements are almost identical. From these calculations one would also expect the overall uranium bands to be similar. In fact, quite the opposite is true. In Fig. 10 we show the fully relativistic total DOS for pure fcc U and Pt. The pure U DOS is clearly different from the U component of UPt_3 (cf. Fig. 5). This is not unexpected since in UPt_3 the uranium atoms have large separations between each other (5.1 Å) compared to their separations in the pure element (3.12 Å in the α-U structure and 3.08 Å in an fcc structure at the same density). Thus, in pure fcc U, the large uranium wave-function overlap causes all of the U states to strongly hybridize with each other. The strongest hybridization occurs between U d and f states, which are difficult to disentangle from each other. The $f_{5/2}$ and $f_{7/2}$ states are also strongly hybridized with each other.

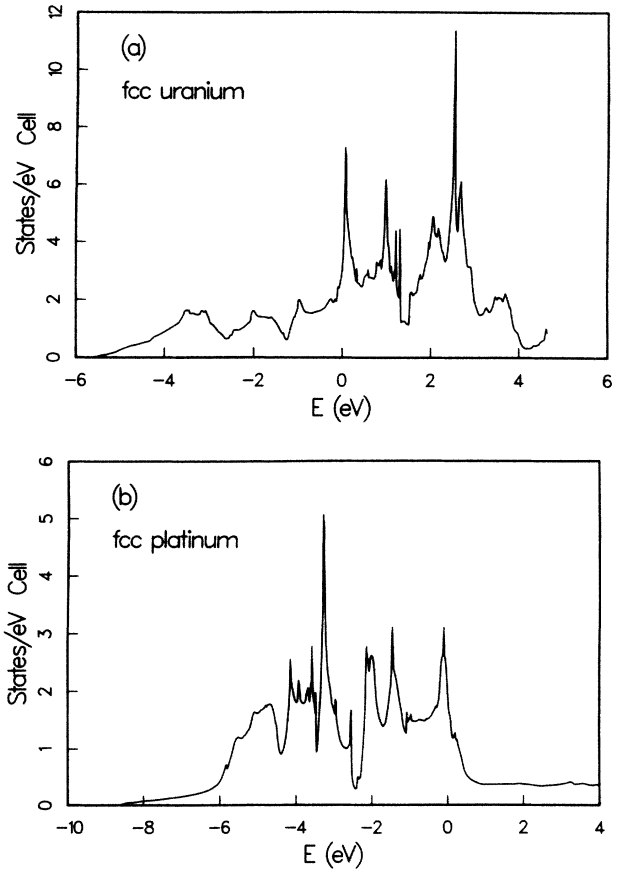

FIG. 10. (a) Pure fcc U total DOS. The energies have been shifted so that the Fermi energy is at zero energy. (b) Pure fcc Pt total DOS. The energies have been shifted so that the Fermi energy is at zero energy.

In UPt_3, on the other hand, there is almost no direct overlap of the uranium d and f orbitals and the uranium projected DOS and structure is determined by the hybridization with the platinum states and hence is quite different from pure uranium. For example, the U d-band hybridization with the platinum d bands results in a moderate U d-band DOS in the region of the Pt d bands (from about 0 to 6 eV below E_F), but pushes the remaining U d character higher in energy. Hence a small U d hybridization gap occurs just above the Pt d bands in the region where the U f bands are located. In general there is almost no hybridization between the different uranium bands in the absence of platinum hybridization. For example, in UPt_3 the uranium $f_{5/2}$ and $f_{7/2}$ components are almost completely decoupled from each other, since the platinum hybridization provides no coupling. In an earlier paper,[28] we have shown by explicit calculation that the U $5f$ hybridization with the platinum $6p$ orbitals is the primary factor controlling the formation of the U $5f$ bands. Similar calculations show that Pt $5d$ hybridization affects the U $6d$ bands most strongly.

Since the electronic structure at the Fermi energy E_F plays such a large role in determining many of the physical properties of metals, it is useful to examine the DOS at E_F. Table I gives the partial DOS contributions (at E_F) from the uranium and platinum sites as well as their percentage contribution to the total DOS per unit cell. For each angular-momentum projection, we have added the two spin-orbit-split components. For example, the d-projected DOS contains both $d_{3/2}$ and $d_{5/2}$ components and the f-projected DOS both $f_{5/2}$ and $f_{7/2}$ components. As expected, most ($\frac{2}{3}$) of the total DOS per unit cell is U $5f$ in character. The next largest projected DOS is of platinum $5d$ character (19%). Since the U $5f$ states must hybridize with the platinum states to form the itinerant

TABLE I. The projected U and Pt density of states at the Fermi energy for UPt_3 in the observed hexagonal $SnNi_3$ crystal structure, normalized per unit cell. The l-projected quantities are sums over the relevant j-projected quantities of the fully relativistic calculations, i.e., $j = l \pm \frac{1}{2}$. For example, f quantities are really sums over $f_{5/2}$ and $f_{7/2}$ quantities. There are two equivalent U sites and six equivalent Pt sites for this crystal structure and the densities of states in this table can be divided by these quantities to obtain results normalized per atom.

	DOS at E_F (states $eV^{-1}cell^{-1}$)	% of total (per cell)
U s	0.04	0%
U p	0.11	1%
U d	0.50	3%
U f	11.40	66%
Pt s	0.50	3%
Pt p	1.02	6%
Pt d	3.34	19%
Pt f	0.34	2%
Total U	12.05	70%
Total Pt	5.20	30%

states that always result from band calculations and since platinum makes up so much of the unit cell, it is not surprising to find a platinum component. The large value for this component (30%) results because the normalization is per unit cell, which contains six Pt atoms and only two U atoms. The total DOS contribution per atom is 35% per U atom and 5% per Pt atom and each U atom gives a contribution to the total DOS at E_F which is 7 times greater than each Pt atom. The total DOS at E_F for the fully relativistic calculations gives 17.25 states/eV cell. This corresponds to a bare linear specific-heat coefficient $\gamma_0=20.3$ mJ(mole U)$^{-1}$K^{-2}. Since the experimental γ is 452 mJ(mol U)$^{-1}$K^{-2}, the specific-heat enhancement is $\lambda=\gamma/\gamma_0=22.3$. Such a huge enhancement factor implies strong electron-electron renormalization of the low-temperature electronic structure.

IV. OTHER ASPECTS OF THE ELECTRONIC STRUCTURE

Because of the large separation between the uranium atoms in UPt_3 the U f states can only become itinerant through hybridization with neighboring atomic orbitals. One simple calculation that can be done to shed some light on this area is to compare calculations where the U f states are placed in the atomic core (which we will refer to as "f-core" calculations) with calculations where the f states are treated as bandlike (which we will refer to as "f-band" calculations). In Fig. 9 we show the DOS for UPt_3 in the $SnNi_3$ structure for self-consistent calculations where we have forced three U f states into the core and included only up to d orbital angular-momentum components in the conduction-band states. Comparing with Figs. 5 and 9, we see that most of the structure (besides the f bands) is similar. This suggests that the U f-core charge contributions to the charge density must be reasonably close to the self-consistent f-band density.

If we carefully examine the projected DOS (not shown here), we find little difference between the two sets of data. The biggest effects due to hybridization with U $5f$ bands are on the U $p_{3/2}$-, Pt $p_{1/2}$-, Pt $p_{3/2}$-, and Pt $d_{5/2}$-projected DOS, where additional structure is seen reflecting the position and structure of the U $5f$ bands, while the projected DOS at other energies is almost identical with the case where the U $5f$ states are put in the core. These results are consistent with some earlier work,[28] where we have shown that platinum p hybridization most directly affects the U $5f$ band while U $5f$ and Pt $5d$ hybridization induces additional Pt d structure above the main part of the Pt $5d$ band.

The most striking difference between Figs. 5 and 9 is the placement of the Fermi energy. In Fig. 5 the Fermi energy is located in the U $5f$ bands, which are above the main part of the Pt $5d$ band. In Fig. 9, the $5f$-core case, the Fermi energy seems to sit at lower energies and cut across the top of the Pt d band, reminiscent of the case for pure fcc Pt metal (cf., Fig. 10). This seems to suggest that more charge transfer from the U to the Pt states occurs when the U $5f$ states are put into the bands and hence fills up the Pt $5d$ band. This point of view, however, is incorrect.

To examine this question more carefully it is useful to attempt to quantify our analysis. In Table II we show the l-projected occupation numbers per atom for different kinds of comparison calculations, including that for UPt_3 in the $SnNi_3$ structure with and without the $5f$ electrons in the core, for UPt_3 in the $AuCu_3$ structure, and for pure fcc U and Pt (at the same atomic-sphere radius of 3.0488 bohrs that was used in the UPt_3 calculations). To get the l-projected quantities we summed over the appropriate spin-orbit split states (e.g., the $f_{5/2}$ and $f_{7/2}$ j components for f-projected quantities). Table II shows that the U d and f occupations are reduced from their pure element counterpart, while the $AuCu_3$ and $SnNi_3$ structure values are all similar. In contrast the l-projected platinum occupation numbers are about the same, whether for the pure metal or for UPt_3 and in either structure ($AuCu_3$ or $SnNi_3$).

It should be noted that these entries are ambiguous in the sense that they depend on the atomic-sphere radii chosen for each atom (how we divide up the space between the uranium and platinum atoms). If, for example, we had expanded the uranium radii and contracted the platinum radii (while keeping the total volume per cell fixed), we would have found different values for the entries in the tables. Instead of using the ratio of the radii as an additional variational parameter to lower the total energy of the system, we have decided to use the same

TABLE II. Total and partial occupations per atom for fully relativistic UPt_3 calculations. The headings $SnNi_3$ and $AuCu_3$ refer to the crystal structure of the calculations. However, the last column (labeled pure fcc U and Pt) give the results for the pure metals at the same average atomic-sphere radius per atom (3.0488 bohrs) as UPt_3. Calculations where the U $5f$ states were treated as bands are labeled $5f$ band and where they are treated as core states as $5f$ core. The lowest rows contain the occupations of the U $6p$ band, divided into the U and Pt contributions. All occupation numbers are normalized per atom and must be multiplied by the number of each type of atom for occupations per unit cell. For example, to get the expected six electrons per U atom for the U $6p$ band, the Pt contribution must be multiplied by 3 and added to the U contribution, since there are three Pt atoms for each U atom.

Structure	$SnNi_3$ $5f$ band	$SnNi_3$ $5f$ core	$AuCu_3$ $5f$ band	Pure fcc U and Pt
U s	0.36	0.36	0.36	0.49
U p	0.38	0.38	0.36	0.18
U d	1.57	1.45	1.44	2.31
U f	2.69		2.74	3.02
Total	4.99	2.19	4.90	6.00
Pt s	0.92	0.86	0.89	0.77
Pt p	0.89	0.79	0.89	0.79
Pt d	8.37	8.62	8.42	8.30
Pt f	0.16		0.16	0.15
Total	10.34	10.27	10.36	10.0
U $6p$ band				
U	5.61	5.58	5.59	
Pt	0.13	0.14	0.14	

atomic radii (3.0488 bohrs) for all atoms in all structures. Besides making intercomparisons between different structures easier, this prescription also has the virtue of minimizing the fraction of cell volume in which two or more atomic spheres overlap.

If we compare the l occupation numbers in Table II for the $5f$-core and $5f$-band cases, we find only a small difference in the charge transfer (an additional 0.2 electron per U atom or 0.07 electron per Pt atom for the $5f$-band case). Moreover, the Pt d occupation is also similar (increasing by only 0.25 d electrons per Pt atom when the U $5f$'s are placed in the core). Most surprising of all is that the platinum d occupation is actually smaller when the Fermi level is above the filled d band (U $5f$'s as bands) than when the Fermi level is in the top of the d bands (U $5f$'s as core states).

This paradox arises because of the ambiguity in determining the exact bottoms and tops of any pure l band for hybridized electronic systems, since hybridization allows mixing of different l-dependent states. This is clearly shown in Figs. 6 and 7, where hybridization removes some of the intensity from the main part of the U $5f$ and Pt $5d$ bands and shifts part of the projected DOS to other energies. If we arbitrarily define the top of the Pt d band to be just above the main part of the d band, then the filled $5d$ band in pure fcc Pt metal [Fig. 10(b)] contains 8.9 Pt d electrons per Pt atom. For UPt_3 with the U $5f$ electrons in the core (Fig. 9), there are 8.8 Pt d electrons per Pt atom, and for UPt_3 with the U $5f$'s as bands there are 8.2 Pt d electrons per Pt atom in the filled Pt $5d$ band. These numbers then suggest the following interpretation: In UPt_3 the Pt $5d$ band would normally be similar to the pure fcc metal band (at the same average atomic-sphere radius). However, hybridization with the U $5f$ bands induce additional structure in the Pt d states that in turn are taken from the top of the platinum d bands, which is why the Fermi energy seems to be above the main part of the Pt d band for the $5f$-band case. The d electron states that have been removed show up as the induced d states in the projected Pt d DOS that is above the apparent top of the $5d$ band. Because E_F is near the bottom of the U $5f$ bands, some of these induced Pt d states are unoccupied, causing the Pt d electron occupation to drop slightly.

Besides hybridization effects with the U f states, the local symmetry around each f atom could also be important for understanding differences in heavy-fermion behavior. To test for these kinds of sensitivities, we have done comparison calculations for UPt_3 in the $AuCu_3$ structure, and in Fig. 11 show the resulting total DOS. Comparing Figs. 5 and 11, it is clear that the gross features of the band structures are similar. Because of the symmetry constraints on the bands due to the underlying crystal structure, however, fine details in the total DOS can be significantly altered, especially near E_F. These fine details, which would not matter much in an ordinary metal, can be strongly amplified for heavy-fermion materials because the f-atom bands are so flat. Hence, even tiny shifts in these bands greatly affect the DOS near E_F. In Fig. 12 we see that for UPt_3 in the $SnNi_3$ structure, E_F is located near a relative minimum in the f-band DOS, whereas in

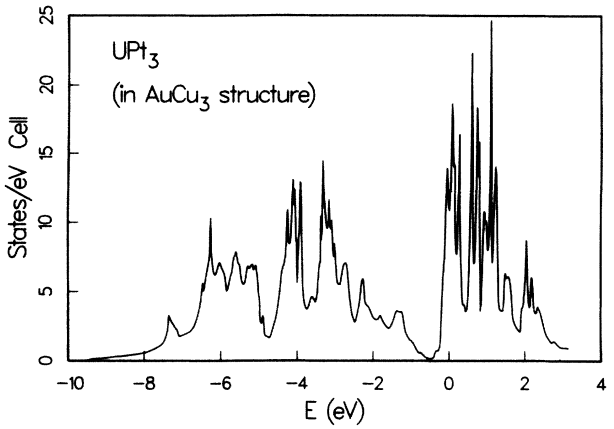

FIG. 11. Total DOS for UPt_3 in the $AuCu_3$ structure. The energies have been shifted so that the Fermi energy is at zero energy.

the $AuCu_3$ structure it is found to be near a maximum. This may possibly tend to favor the $SnNi_3$ structure over the $AuCu_3$ structure.

The most obvious difference to the eye between the DOS of UPt_3 in the two structures (Figs. 5 and 11) is a gap in the DOS of about $\frac{1}{2}$ eV, which opens up between the top of the main part of the Pt $5d$ band and the bottom of the U $5f$ band for the $AuCu_3$ structure. In the $SnNi_3$ structure these two bands are almost touching. From Table II this seems to have almost no effect on either the l-projected occupation numbers or, as we shall see later, the partial pressures. Because the Pt $5d$ band is slightly further away from the U $5f$ band, however, the amount of U $5f$ character in the long low energy tail below the top of the Pt d band (cf. Fig. 6) due to hybridization is slightly reduced (from 1.5 U $5f$ electrons per U atom to 1.1 electrons per U atom). The number of Pt d electrons in the main part of the Pt $5d$ band for the $AuCu_3$ structure (8.33 d electrons per Pt atom) is similar to that in the $SnNi_3$ structure. A summary is as follows: except for

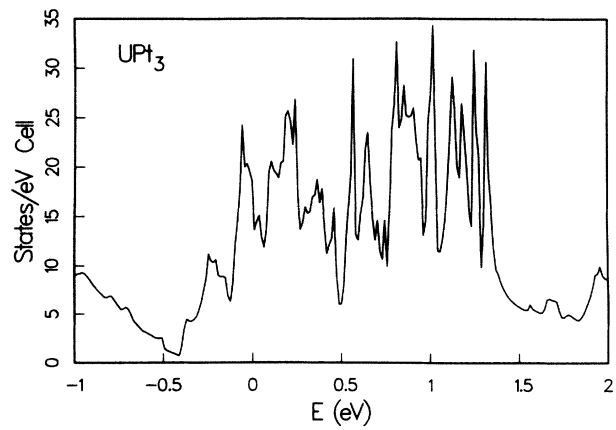

FIG. 12. Blow up of the total DOS near E_F for the $SnNi_3$ crystal structure. The energies have been shifted so that the Fermi energy is at zero energy.

changes in the DOS (especially at E_F), whether the underlying symmetry is hexagonal ($SnNi_3$ structure) or cubic ($AuCu_3$ structure) seems to play little role in most of the one-electron properties of UPt_3.

Because of the sensitivities in the f-band DOS at E_F, we have tested how the band structure changes when a different exchange correlation potential is used. For this comparison we have used the exchange-only $X\alpha$ ($\alpha=\frac{2}{3}$) local exchange potential. When compared to the results for the Barth-Hedin exchange-correlation potential that is used for all of the other calculations in this paper, we find almost no differences in the total DOS or the projected DOS, even near E_F. The l-projected occupation numbers per atom for the U s, p, d, f conduction bands are 0.37, 0.39, 1.68, 2.58 and for the Pt s,p,d,f conduction bands are 0.93, 0.95, 8.28, 0.17, respectively. These are similar to the l-projected occupation numbers that were obtained from the Barth-Hedin potential, which are listed in Table II.

V. BONDING PROPERTIES

One simple property of any material is its bonding properties, which can be studied by examining the equilibrium lattice spacing and bulk modulus. Band-structure models offer a clear prediction of bonding properties,[49,50] and have been successfully applied to f-electron systems[51] and even more successfully to transition metals, although it is worth noting that the local-density exchange-correlation potentials have at times seemed to overestimate the strength of the f bonding.[52]

In contrast, another popular approach for describing heavy-fermion systems is the concentrated Kondo lattice.[14,23,53–57] In this approach the f electrons sit on localized sites at an energy ϵ_f below the Fermi energy E_F. Through hybridization with the normal conduction-band states, a Kondo resonance at E_F may develop and play an important role in the low-temperature properties of such a system. As far as we know, there is no theory to predict bonding properties of the Kondo lattice model.

Without resorting to complicated theoretical models, we can easily gain some simple understanding of the bonding properties in UPt_3 by comparing atomic volumes. In the absence of any strong chemical interaction between the uranium and platinum atoms, according to Vegard's law one would naively expect the equilibrium volume per unit cell of UPt_3 (V_{UPt_3}) to be the sum of the equilibrium atomic volumes of the pure uranium and platinum metals, i.e., $V_{UPt_3}=2(V_U+3V_{Pt})$. The factor of 2 occurs because there are two formula units of UPt_3 per unit cell. Thus, with $V_U=140$ bohrs^3 and $V_{Pt}=102$ bohrs^3, Vegard's law would predict the volume to be 892 bohrs^3. This should be compared with the experimental volume of 950 bohrs^3. For eight Pt atoms the volume would be 816 bohrs^3. Thus UPt_3 has a 6.5% larger volume per cell than we would expect simply from adding the larger uranium atoms.

One possible explanation for the larger volume is that the f-electron bonding of the U atoms is lost when diluted by the platinum matrix. Alternatively, one could argue that the uranium atoms reduce the d-band bonding of the platinum atoms. We can examine these questions both by directly comparing the UPt_3 angular decomposed partial pressures with those of the pure elements as well as by

TABLE III. Partial pressure contributions to the bonding of UPt_3 in kbars. Most of the labels follow the same conventions as Table II. The fully relativistic results are labeled by fully rel and the semirelativistic results (i.e., no spin-orbit coupling) by semirel. The l-projected pressures are sums over the relevant j-projected pressures for the fully relativistic results as in Table I. The contribution from the broadened U 6p core states (treated as a band) are also presented as well as the Madelung contribution to the pressure.

Structure	$SnNi_3$ fully rel 5f band	$SnNi_3$ fully rel 5f core	$AuCu_3$ fully rel 5f band	$SnNi_3$ semirel 5f band
U s	58.1	60.9	60.1	58.2
U p	164.1	166.0	156.5	169.8
U d	−134.8	−125.7	−134.7	−133.0
U f	−160.9		−140.8	−168.0
Total	−73.5	101.2	−58.9	−73.0
Pt s	82.9	71.7	74.1	89.8
Pt p	67.0	56.7	75.1	69.4
Pt d	−79.0	80.4	−63.8	−60.6
Pt f	−67.8		−65.9	−68.4
Total	3.1	208.8	19.5	30.2
U 6p band	−98.2	−102.2	−103.5	
Madelung	−77.3	−59.3	−86.3	−62.3
Total	−245.9	148.5	−229.2	−105.1

comparisons with model calculations where three U f electrons per U atom are forced into the core and not allowed to bond. In Table III the corresponding partial pressures are shown. It is seen that for these quantities the changes due to different kinds of hybridization show up quite strongly. By way of comparison, pure fcc Pt at this same average atomic volume has large negative pressures for all l components (total pressure $=-451$ kbars), since it would like to contract to its equilibrium volume (corresponding to $S=2.897$ bohrs). Pure fcc U at the same UPt_3 average atomic-sphere radius of 3.0488 bohrs has a positive pressure of 184.9 kbars, since it would like to expand to its equilibrium volume ($S=3.221$ bohrs).

From Table III, one sees that both uranium and platinum d and f conduction bands are bonding (have negative partial pressures), while both U and Pt s and p conduction bands are repulsive or antibonding (have positive partial pressures). For the calculations in the $SnNi_3$ structure (the experimentally observed structure), we find the total calculated pressures to be about -250 kbars at the experimental equilibrium lattice constant, about equally divided between the U conduction band, the U $6p$ band, and the Madelung contributions. The Pt conduction-band partial pressure is nearly zero for the sphere radii we have chosen. If we compare the first and fourth columns of Table III, we find that the semirelativistic calculations are remarkably similar to the fully relativistic calculations for almost every partial pressure (the totals are somewhat different since the semirelativistic results did not treat the U $6p$ states as bands and hence are missing this contribution to the pressure). Thus spin-orbit effects seem to play a minor role in the bonding. Also, if we compare columns one and three of Table III, we find that crystal structure seems to only slightly change the bonding properties, since the calculations for both the hexagonal $SnNi_3$ structure and the cubic $AuCu_3$ structure are so similar in all categories. The exchange-only potential did give different results for the partial pressures. The U s,p,d,f conduction-band partial pressures were 66.5, 176.8, -122.6, -161.2 kbars for a total U conduction-band pressure of -40.5 kbars. The Pt conduction band s,p,d,f partial pressures were 109.2, 118.7, -39.9, -61.8 kbars for a total Pt conduction-band pressure of 126.2 kbars. The total U $6p$ band and Madelung contributions were -91.2 and -75.8 kbars. The total pressure for the exchange-only calculations were -81.3 kbars, which is much closer to experiment than the -245.9 kbars of the Barth-Hedin calculations.

Besides this sensitivity to the exchange-correlation potential, the major differences in Table III occur between the first two columns, which compare calculations where the U $5f$ states are treated as band states or as core states. The first difference between these two sets of calculations is the absence of f partial pressures in the f-core results, since core states do not contribute to the pressure. The combined U and Pt f partial pressures in column one of Table III are -228.7 kbars. If we neglect these contributions, we still find the f-band results to have a total pressure of 165.7 kbars lower than the f-core results, primarily due to changes in the Pt d conduction-band partial pressures. The f-core results have a repulsive Pt d contribution of 80.4 kbars, while the f-band results have a bonding or attractive Pt d contribution of -79.0 kbars.

To understand why this change occurs, it is useful to examine the following approximate partial pressure formula,[50,30,58] for the "central pressures" P_c for each band:

$$3P_c\Omega = n\left[\left[-\frac{\delta C}{\delta \ln S}\right]+(\langle E\rangle - C)\left[-\frac{\delta \ln W}{\delta \ln S}\right]\right]. \quad (1)$$

Here Ω is the volume per cell, n is the number of electrons per cell for each component, C is the energy of the center of the band, S is the atomic-sphere radius, $\langle E\rangle$ is the center of gravity of the occupied part of the band, and W is the approximate width of the band. This formula is usually derived in the nonrelativistic (or semirelativistic) limit, where each l-band partial pressure is separately calculated from the above expression (more detailed formulas in terms of the Andersen potential parameters are given in Refs. 50, 30, and 58). A slightly different "tail pressure" P_t formula is actually more accurate for s-p bands, while occupied d-f bands are usually better treated by P_c. The fully relativistic expression turns out[33,38] to be identical to the normal formula if small corrections are neglected and if, instead of sums over the different l bands, one sums over the different κ (or $j=l\pm\frac{1}{2}$) components for each type of atom in the compound. The n, C, $\langle E\rangle$, and W are therefore the relevant quantities for each different κ and atom type.

The intuitive physical understanding of the central pressure formula is very simple. The first term is the change in partial pressure due to a change in the center-of-band energy with a change in volume, while the second term is due to changes in the bandwidth under compression or expansion. They can be derived by writing the one-electron band energy E in the canonical form

$$E = C + \left[\frac{E-C}{W}\right]W. \quad (2)$$

Here $(E-C)/W$, which plays the same role as the factor $(\langle E\rangle - C)/W$ in Eq. (1), is a band-filling factor. If the center of gravity of the occupied part of the band equals the center of the band, then the band is usually completely filled and hence is neither bonding nor antibonding and gives no pressure contribution. If this factor is negative, the band is only partially filled and bonding. Any increase in the bandwidth then makes this contribution more pronounced.

In Table IV we list the important factors of Eq. (1) for the Pt d bands in UPt_3 both for the $5f$-band calculations as well as the $5f$-core calculations. The quantities P_{c_1} and P_{c_2} are given by

$$P_{c_1} = \frac{n}{3\Omega}\left[-\frac{\delta C}{\delta \ln S}\right] \quad (3)$$

and

$$P_{c_2} = \frac{n}{3\Omega}(\langle E\rangle - C)\left[-\frac{\delta \ln W}{\delta \ln S}\right]. \quad (4)$$

If we add the Pt $d_{3/2}$ and $d_{5/2}$ contributions, we find that

TABLE IV. Pt d approximate partial pressures. The quantities in this table are the important pieces in evaluating the central pressure approximation for Eqs. (1)–(4). P_{c_1} and P_{c_2} are defined in Eqs. (3) and (4). P_c is the total of the two. In this table we give the separate spin-orbit split d components. The total of the two can be compared with the more exact results in Table III. The labels $5f$ band and $5f$ core are the same notation as used in the previous tables. Pressures are in units of kbars, n in electrons per unit cell, $-\delta C/\delta \ln S$ in atomic-Rydberg units, and $\langle E\rangle - C$ in mRy (10 mRy $=0.14$ eV).

	$5f$ band		$5f$ core	
	Pt $d_{3/2}$	Pt $d_{5/2}$	Pt $d_{3/2}$	Pt $d_{5/2}$
n	21.35	28.88	21.84	29.65
$-\delta C/\delta \ln S$	0.07	0.12	0.09	0.14
$\langle E\rangle - C$	−11.6	−41.4	−2.9	−29.7
$-\delta \ln W/\delta \ln S$	4.52	4.25	4.40	4.13
P_{c_1}	79.1	179.6	98.1	211.9
P_{c_2}	−57.9	−262.0	−14.4	−187.7
P_c	21.2	−82.4	83.7	24.2

their sum is −61.2 and 107.9 kbars for the $5f$-band and $5f$-core cases in Table IV. If we compare this to the corresponding quantities in Table III, −79.0 and 80.4 kbars, we see that the approximate formula for P_c is too high by about 20 kbars for both cases and hence is in reasonable agreement. For either table, the $5f$-core Pt d pressure is about 160 kbars higher than the corresponding $5f$-band pressure.

Given this degree of reliability for the approximate pressure formula for P_c, we can attempt to examine the individual factors in Table IV to find the differences caused by the differing treatment of the U $5f$ electrons. From Table IV we find that the occupation numbers and $-\delta \ln W/\delta \ln S$ (the change in the bandwidth under compression) are about the same between the two sets of calculations. About $\frac{1}{3}$ of the increased Pt d pressure that occurs when the U $5f$ states are changed from band to core states is due to P_{c_1}, which reflects the difference in how the d-band center changes with compression. The other $\frac{2}{3}$ of the increase, or the largest part of the increase, is due to P_{c_2} and largely reflects changes in $\langle E\rangle - C$ (the band-filling factor). From a general examination of the Pt d-projected DOS of the two calculations (cf. Figs. 5 and 9), it appears as if the main part of the Pt d bands are about 50 mRy (0.7 eV) lower for the $5f$-band case (relative to the Fermi energy E_F). For both j components the center of the band C (not separately shown in Table IV) is about 40 mRy lower for the $5f$-band case, while the center of gravity $\langle E\rangle$ is about 50 mRy lower. Hence in both cases $\langle E\rangle - C$ is about 10 mRy lower in energy when the U $5f$ electrons are treated as bands. Since the Pt d bands are almost completely filled, $|\langle E\rangle - C|$ is small (≤ 40 mRy) and hence this small change in $\langle E\rangle - C$ has a relatively large effect. This is the reason why the U f with Pt d hybridization, which pushes the main part of the Pt d band to slightly lower energies relative to E_F while pulling off some states from the top of the band, has such a dramatic effect on the Pt d partial pressures.

If we compare the partial pressures of Table III with calculations for pure fcc U and Pt at the same average atomic-sphere radius as UPt_3, as we have discussed earlier, the uranium is compressed and gives positive pressures while the platinum is expanded and gives negative pressures. Because the uranium electronic structure in UPt_3 is largely determined by hybridization with the surrounding platinum atoms, the pure fcc U partial pressures are different from that in UPt_3. Because the uranium concentration ($\frac{1}{4}$) is also so large, the platinum partial pressures are also very different. Thus, in regard to our earlier discussion of the larger than expected volume of UPt_3, it is clear that this can neither be ascribed to the breaking up of the f-electron bonding of the U atoms nor that of the Pt d-band bonding. The uranium and platinum atoms interact too strongly for either description to have much relevance. This strong interaction also explains why the simple Vegard's-law geometrical scaling of atomic sizes also fails to reproduce the observed equilibrium volume of UPt_3.

VI. COMPARISON OF UPt_3 WITH UIr_3 AND UAu_3

We can gain further insight into the Pt d and U f interaction by comparing UPt_3 with UIr_3 and UAu_3, i.e., compounds where we have replaced Pt by its neighboring elements ($Z\pm 1$). We have done these additional calculations in the $AuCu_3$ structure at the same average atomic-sphere radius as for the UPt_3 calculations. The UIr_3 compound actually forms in this structure, but at an equilibrium volume 8% smaller than our calculations. The structure of UAu_3 is not known experimentally, but is probably not the $AuCu_3$ structure. By examining UIr_3 and UAu_3 we are subtracting or adding electrons and hence tuning across the top of the transition-metal $5d$ band.

While our main emphasis in this section is on the transition-metal d interactions with the U f states, one should not forget that the transition-metal p states also play an active role. This is most easily seen by performing the same kind of LMTO calculations that selectively turned on and off different kinds of hybridization as was done for UPt_3 in Ref. 28. From these types of calculations we have found that hybridization with the transition-metal p states plays the dominant role in the formation of the U f band for UPt_3 and UAu_3. For UIr_3 the situation is more complex, since the hybridization with the Ir d states is almost as effective as that of the Ir p states in the formation of the U f band. As was found in Ref. 28 the effects of hybridization are often unsymmetrical. While for UPt_3 and UAu_3 the transition-metal d and U f hybridization has only minor effects on the U f states, this same hybridization has a much stronger effect on the transition-metal d states by inducing new structure above the main part of the d bands that would otherwise be absent. For UIr_3, on the other hand, since the Ir d and U f bands overlap and interact so strongly, the effects of hybridization are more equal on both types of states.

The total DOS of the fully relativistic, self-consistent calculations for UIr_3 and UAu_3 are shown in Figs. 13(a) and 13(b). These should be compared with the results for

UPt_3 in the $AuCu_3$ structure, Fig. 11. For UIr_3 the U $5f$ bands are located in the top of the Ir $5d$ bands and the two bands strongly interact.[59] The UPt_3 situation is a borderline case, where the interactions are still strong, but where the U $5f$ interaction just barely manages to pull off some of the d states from the top of the $5d$ band. For UAu_3 the d-f interaction has been greatly decreased and the U $5f$ bands are well above the main part of the Au d band.

The transition-metal d-projected DOS as well as their effect on the $N_{6,7}$ soft x-ray emission spectra of Ir, Pt, and Au were given in an earlier publication.[60] These results confirm the discussion presented in the above paragraph. We can complement them with the U f-projected DOS for UIr_3, UPt_3, and UAu_3 in the $AuCu_3$ structure, which are presented in Figs. 14(a), 14(b), and 14(c). As might be expected, the greatest transition-metal d with U f interactions occur between the nearest subcomponent bands, i.e., the transition-metal $5d_{5/2}$ and U $5f_{5/2}$ bands. For UIr_3 the U $5f_{5/2}$ projected DOS shows a pronounced tail below the main part of the U $5f$ band [i.e., for energies less than 0 in Fig. 14(a)], which is a direct confirmation of the strong d-f hybridization. In UPt_3 this tail, while still visi-

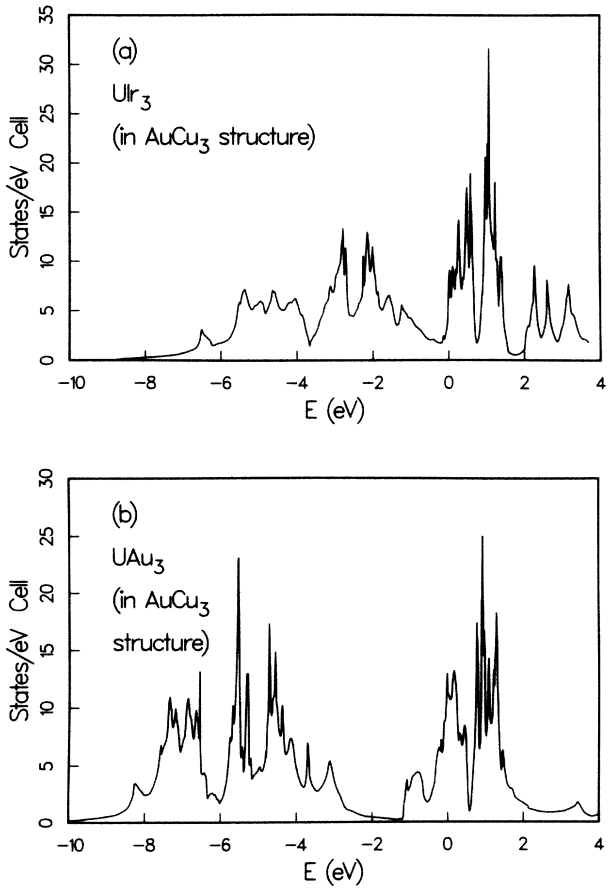

FIG. 13. (a) Total DOS for UIr_3 in $AuCu_3$ structure ($S_{av}=3.0488$ bohrs). The energies have been shifted so that the Fermi energy is at zero energy. (b) Total DOS for UAu_3 in $AuCu_3$ structure ($S_{av}=3.0488$ bohrs). The energies have been shifted so that the Fermi energy is at zero energy.

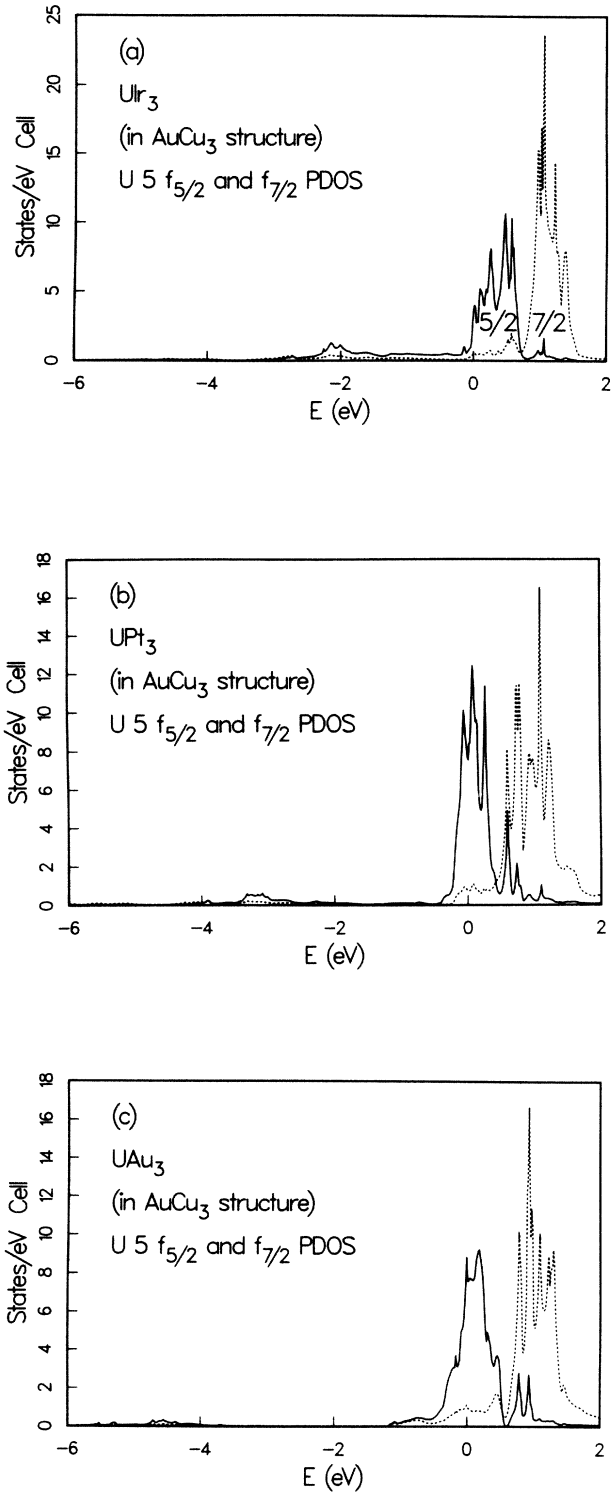

FIG. 14. (a) The $\frac{5}{2}$ (solid line) and $\frac{7}{2}$ (dashed line) j components of the U $5f$ PDOS for UIr_3 in the $AuCu_3$ structure. The energies have been shifted so that the Fermi energy is at zero energy. (b) The $\frac{5}{2}$ (solid line) and $\frac{7}{2}$ (dashed line) j components of the U $5f$ PDOS for UPt_3 in the $AuCu_3$ structure. The energies hae been shifted so that the Fermi energy is at zero energy. (c) The $\frac{5}{2}$ (solid line) and $\frac{7}{2}$ (dashed line) j components of the U $5f$ PDOS for UAu_3 in the $AuCu_3$ structure. The energies have been shifted so that the Fermi energy is at zero energy.

ble, is small. In UAu_3 the tail is slightly smaller than for UPt_3, and pushed even further below the U $5f$ band. Hence UPt_3 seems qualitatively closer to UAu_3 than to UIr_3, with a larger separation in energy between the transition-metal d band and the U $5f$ band for UAu_3 than for UPt_3. These effects are also seen in the transition-metal d-projected DOS.[60] In the region of energy of the U $5f$ bands, there is distinct structure in the transition-metal d-projected DOS that mirrors the U $5f$ bands. This induced transition-metal d structure is in the top of the main part of the d band and very pronounced in UIr_3. In UPt_3 it is just barely above the main part of the Pt d band, but while weaker than for UIr_3 is still reasonably strong. In UAu_3 this structure is small and far above the main part of the d band.

These effects also show up in the placement of the Fermi energy E_F, which is always in the U $f_{5/2}$ band. In UIr_3 the Fermi energy E_F is much closer to the bottom of the f band than for the other two compounds, which are more similar to each other in this respect. This is only slightly due to fewer U $5f$ electrons (2.48, 2.74, and 2.65 electrons per U atom for UIr_3, UPt_3, and UAu_3). It is mainly due to the long tail in the U f-projected DOS that contains most of the U $5f$ electrons (about 2.25 electrons) in UIr_3, whereas most of the occupied U $5f$ states in UPt_3 and UAu_3 are in the main part of the U $5f$ bands.

VII. SUMMARY AND DISCUSSION

We have presented detailed results on the one-electron properties of UPt_3 as well as comparisons to other relevant calculations. We have shown that the basic electronic band structure of UPt_3 is composed of a narrow spin-orbit split U $5f$ band at E_F, which is just above a filled Pt $5d$ band. Some states have been removed from the top of this band by Pt d and U f hybridization to form a reasonably large induced Pt d DOS in the region of the U $5f$ bands (which are at E_F) and just above the main part of the Pt $5d$ bands. The broad U $6d$ states, which normally hybridize strongly with the U $5f$ states in pure uranium, have some DOS weight in the energy region of the Pt $5d$ bands, but are otherwise pushed to higher energies by the Pt d hybridization and hence begin to turn on strongly at energies just above the U $5f$ bands. In the background of the DOS are broad U $7s$ and Pt $6s$-$6p$ bands. Hybridization with the Pt p states is the primary factor controlling the width of the U $5f$ bands. The U $7p$ and Pt $5f$ bands are well above E_F and are largely irrelevant to the basic electronic structure.

Comparison calculations where we have forced three U $5f$ electrons into the core and calculated the remaining band structure with an s-p-d basis have confirmed that the dramatic change in the top of the Pt $5d$ band is caused by U f and Pt d hybridization. The presence or absence of itinerant U f electrons therefore has an important impact on the electronic structure. Any experiment that can probe the Pt d structure could provide some useful experimental insight. It would also be of interest to know whether Kondo-lattice-type theories could also so radically change the Pt d electronic structure.

We have also attempted to analyze the electronic structure of UPt_3 from equilibrium bonding or partial pressure calculations. The respective projected electronic structure is very different than pure fcc uranium and platinum and a Vegard-law analysis confirms that U and Pt interact strongly in UPt_3. Like most density-functional calculations, we find too much bonding, with a total pressure of -246 kbars at the equilibrium lattice constant for calculations with the Barth-Hedin exchange-correlation potential. The exchange-only calculations, however, give a much better pressure (-81.3 kbars). A partial pressure decomposition shows the U and Pt d-f states to be bonding while the U and Pt s-p states are repulsive or antibonding. Forcing three U $5f$ bandlike states into the U atomic core increases the pressure by 394 kbars. This large increase reflects not only the loss of f bonding, but also the change in the Pt d partial pressure from bonding to antibonding due to the modifications in the Pt d band electronic structure when the U f hybridization is not present. In general, the full band-structure calculation of the pressure at the experimental equilibrium volume is too strongly bonding. However, if we note the uncertainty due to exchange-correlation potential effects and that most density-functional calculations of bonding tend to overbond, especially for more localized states such as the U $6p$-core band and the U $5f$ band, and reflect on the enormous increase in pressure that occurs if we force the U f electrons into the core, our overall conclusion tends to suggest that itinerant U $5f$ states are necessary to obtain the correct equilibrium lattice constant.

We have also performed comparison calculations of neighboring UIr_3 and UAu_3 at the same average atomic volume and in the $AuCu_3$ crystal structure in order to change the placement of the U $5f$ bands from being in the top of the main part of the transition-metal d band to being well above it. We find that this greatly affects the hybridization between the U f and transition-metal d states. In UIr_3 this hybridization is strong and causes the total DOS at E_F to be greatly reduced and the f-band DOS to have a large tail, which is well below the main part of the U $5f$ band and contains most of the occupied U f electrons. In contrast, this hybridization for UPt_3 and UAu_3 is much weaker, with most of the occupied U $5f$ bands above the main part of the transition-metal d band. The electronic structure of both materials is similar and through hybridization both induce transition-metal d contributions in the region of the U $5f$ bands. However, because the U $5f$ bands are closer in energy to the d bands in UPt_3, the induced transition-metal d structure is correspondingly larger for UPt_3 than for UAu_3.

Because of the strong enhancements that are seen experimentally, in the specific heat for example, UPt_3 seems to be a clear-cut example of a system whose low-temperature properties demand the inclusion of strong many-body correlations in the electronic structure to achieve a proper understanding. Nonetheless, because of the complexities and differences seen in all heavy-fermion materials, a realistic treatment of hybridization and other aspects of the electronic structure that are not usually included in many-body models but are treated by one-electron band-structure calculations are also probably essential to make sense of the physical properties of this unusual material.

In this paper we have tried to present as clear a picture as we could of the hybridization and one-electron properties of UPt_3. Our results are probably most applicable to the non-f-band electrons in the system. Despite this, the model f-core band-structure comparison calculations seem to strongly suggest that whatever strongly interacting form the U $5f$ states condense into they must have some itinerant character to provide the proper bonding. Moreover, whether or not the f electrons are local or itinerant has strong implications for the structure of the Pt d bands, which one should be able to probe experimentally. In conclusion, we believe that a full understanding of the low-temperature properties will probably only be accomplished after a suitable theory is developed that can simultaneously handle the f-band many-body correlations together with the important hybridizations to the more normal electronic structure.

*Present address.

[1]P. H. Frings, J. J. M. Franse, F. R. de Boer, and A. Menovsky, J. Magn. Magn. Mater. **31-34**, 240 (1983).

[2]G. R. Stewart, Z. Fisk, J. O. Willis, and J. L. Smith, Phys. Rev. Lett. **52**, 679 (1984).

[3]P. Strange and B. L. Gyorffy, Physica **130B**, 41 (1985).

[4]A. M. Boring, R. C. Albers, F. M. Mueller, and D. D. Koelling, Physica **130B**, 171 (1985).

[5]J. Sticht and J. Kübler, Solid State Commun. **54**, 389 (1985).

[6]R. C. Albers, A. M. Borning, and N. E. Christensen, Bull. Am. Phys. Soc. **30**, 523 (1985).

[7]T. Oguchi and A. J. Freeman, Bull. Am. Phys. Soc. **30**, 356 (1985).

[8]T. Oguchi and A. J. Freeman, J. Magn. Magn. Mater. **52**, 174 (1985).

[9]G. R. Stewart, Rev. Mod. Phys. **56**, 755 (1984).

[10]G. Aeppli, E. Bucher, and G. Shirane, Phys. Rev. B **32**, 7579 (1985).

[11]W. J. L. Buyers, J. K. Kjems, and J. D. Garrett, Phys. Rev. Lett. **55**, 1223 (1985).

[12]H. R. Ott, H. Rudigier, Z. Fisk, and J. L. Smith, Phys. Rev. Lett. **50**, 1595 (1983).

[13]H. R. Ott, H. Rudigier, T. M. Rice, K. Ueda, Z. Fisk, and J. L. Smith, Phys. Rev. Lett. **52**, 1915 (1984).

[14]P. W. Anderson, Phys. Rev. B **30**, 1549 (1984).

[15]P. W. Anderson, Phys. Rev. B **30**, 4000 (1984).

[16]W. D. Schneider and C. Laubschat, Phys. Rev. B **23**, 997 (1981).

[17]J. J. M. Franse, J. Magn. Magn. Mater. **31-34**, 819 (1983).

[18]K. Scharnberg and R. A. Klemm, Phys. Rev. Lett. **54**, 2445 (1985).

[19]F. Steglich, J. Aarts, C. D. Bredl, W. Lieke, D. Meschede, W. Franz, and J. Schäfer, Phys. Rev. Lett. **43**, 1892 (1979).

[20]G. R. Stewart, Z. Fisk, and J. O. Willis, Phys. Rev. B **28**, 172 (1983).

[21]J. W. Chen, S. E. Lambert, M. B. Maple, Z. Fisk, J. L. Smith, G. R. Stewart, and J. O. Willis, Phys. Rev. B **30**, 1583 (1984).

[22]D. J. Bishop, C. M. Varma, B. Batlogg, E. Bucher, Z. Fisk, and J. L. Smith, Phys. Rev. Lett. **53**, 1009 (1984).

[23]F. Steglich, U. Ahlheim, J. J. M. Franse, N. Grewe, D. Rainer, and U. Rauchschwalbe, J. Magn. Magn. Mater. **52**, 54 (1985).

[24]Z. Fisk, H. R. Ott, and J. L. Smith, J. Magn. Magn. Mat. **47-48**, 12 (1985).

[25]G. P. Meisner, A. L. Giorgi, A. C. Lawson, G. R. Stewart, J. O. Willis, M. S. Wire, and J. L. Smith, Phys. Rev. Lett. **53**, 1829 (1984).

[26]H. H. Hill, in *Plutonium 1970*, edited by W. N. Miner (Metallurgical Society of the AIME, New York, 1970), p. 2.

[27]D. D. Koelling, B. D. Dunlap, and G. W. Crabtree, Phys. Rev. B **31**, 4966 (1985).

[28]R. C. Albers, Phys. Rev. B **32**, 7646 (1985).

[29]O. K. Andersen, Phys. Rev. B **12**, 3060 (1975).

[30]H. L. Skriver, *The LMTO Method* (Springer, Berlin, 1984).

[31]N. E. Christensen, J. Phys. F **8**, L51 (1978).

[32]N. E. Christensen, Solid State Commun. **44**, 51 (1982).

[33]N. E. Christensen and J. W. Wilkins, Phys. Scr. **25**, 691 (1982).

[34]M. S. S. Brooks, J. Phys. F **13**, 103 (1983).

[35]M. S. S. Brooks, J. Phys. F **14**, 639 (1984).

[36]M. S. S. Brooks, J. Phys. F **14**, 653 (1984).

[37]M. S. S. Brooks, J. Phys. F **14**, 857 (1984).

[38]N. E. Christensen, Int. J. Quant. Chem. **25**, 233 (1984).

[39]C. Godreche, J. Magn. Magn. Mater. **29**, 262 (1982).

[40]V. V. Nemoshkalenko, A. E. Krasovskii, V. N. Antonov, Vl. N. Antonov, U. Fleck, H. Wonn, and P. Ziesche, Phys. Status Solidi B **120**, 283 (1983).

[41]V. V. Nemoshkalenko, A. E. Krasovskii, V. N. Antonov, Vl. N. Antonov, U. Fleck, H. Wonn, and P. Ziesche, Phys. Status Solidi B **123**, 787 (1984).

[42]U. von Barth and L. Hedin, J. Phys. C **5**, 1629 (1972).

[43]O. Jepsen and O. K. Andersen, Solid State Commun. **9**, 1763 (1971).

[44]G. Lehman and M. Taut, Phys. Status Solidi **54B**, 469 (1972).

[45]T. J. Heal and G. I. Williams, Acta Crystallogr. **8**, 494 (1955).

[46]B. Roof (private communication).

[47]M. E. Rose, *Relativistic Electron Theory* (Wiley, New York, 1961).

[48]H. L. Skriver, Phys. Rev. B **14**, 5187 (1976).

[49]V. L. Moruzzi, J. F. Janak, and A. R. Williams, *Calculated Electronic Properties of Metals* (Pergamon, New York, 1978).

[50]A. R. Mackintosh and O. K. Andersen, in *Electrons at the Fermi Surface*, edited by M. Springford (Cambridge University Press, Cambridge, 1980), pp. 149–224.

[51]H. L. Skriver, O. K. Andersen, and B. Johansson, Phys. Rev. Lett. **41**, 42 (1978).

[52]D. Glötzel, J. Phys. F **8**, L163 (1978).

[53]H. Razafimandimby, P. Fulde, and J. Keller, Z. Phys. B **54**, 111 (1984).

[54]N. d'Ambrumenil and P. Fulde, J. Magn. Magn. Mater. **47-48**, 1 (1985).

[55]M. Tachiki and S. Maekawa, Phys. Rev. B **29**, 2497 (1984).

[56]S. Horn, E. Holland-Moritz, M. Loewenhaupt, F. Steglich, E. Scheuer, A. Beneit, and J. Floquet, Phys. Rev. B **23**, 3171 (1981).

[57]A. Yoshimori and H. Kasai, J. Magn. Magn. Mater. **31-34**, 475 (1983).

[58]N. E. Christensen and V. Heine, Phys. Rev. B **32**, 6145 (1985).

[59]A. J. Arko, D. D. Koelling, and B. Reihl, Phys. Rev. B **27**, 3955 (1983).

[60]R. C. Albers, A. M. Boring, P. Weinberger, and N. E. Christensen, Phys. Rev. B **32**, 7571 (1985).